DOI: 10.1002/cphc.200700655

Fluorescence Nanoscopy with Optical Sectioning by Two-Photon Induced Molecular Switching using Continuous-Wave Lasers

Jonas Fölling,[a] Vladimir Belov,[a] D. Riedel,[b] Andreas Schönle,[a] Alexander Egner,[a] Christian Eggeling,*[a] Mariano Bossi,*[a] and Stefan W. Hell[a]

During the last decade far-field fluorescence microscopy methods have evolved that have resolution far below the wavelength of light. To outperform the limiting role of diffraction, all these methods, in one way or another, switch the ability of a molecule to emit fluorescence. Here we present a novel rhodamine amide that can be photoswitched from a nonfluorescent to a fluorescent state by absorption of one or two photons from a continuous-wave laser beam. This bright marker enables strict control of on/off switching and provides single-molecule localization precision down to 15 nm in the focal plane. Two-photon induced nonlinear photoswitching of this marker with continuous-wave illumination offers optical sectioning with simple laser equipment. Future synthesis of similar compounds holds great promise for cost-effective fluorescence nanoscopy with noninvasive optical sectioning.

Introduction

Since Abbe's seminal work[1] on image formation in lens-based optical microscopy, it has been widely accepted that the resolution of a microscope employing propagating beams of light is limited by diffraction. However, in the early 1990s it was discovered that, in far-field fluorescence microscopy, the diffraction barrier can be overcome if the fluorophore properties, in particular the ability of a molecule to reside in different states, is judiciously incorporated into the imaging process.[2] Henceforth, every far-field optical microscopy concept that has successfully outperformed diffraction is based on the use of (at least) two molecular states, one of which is dark while the other gives a signal.[3] Although the bright state need not be fluorescent, the use of fluorescence as a messenger signal brings about high molecular sensitivity and specificity.

The first subdiffraction concepts following this pathway utilized a reversible saturable transition or even photoswitching between a fluorescent and a nonfluorescent state with a beam of light featuring a local intensity minimum.[3–7] Reversibly confining the signal to the very proximity of the minimum breaks the diffraction barrier. The archetype of these concepts, stimulated emission depletion microscopy,[4] has reached focal-plane resolution down to 16 nm,[8,9] although spatial resolution of the size of a molecule is conceptually possible. The same strategy can be realized by reversibly photoswitching suitable fluorophores between a dark and a bright (meta)stable state.[5,10–12] In all these concepts, the fluorescent labels are forced to undergo several cycles between the bright and the dark state. Unfortunately, the number of switching cycles of a molecule is limited by switching fatigue.

Multiple switching is elegantly avoided by photoswitching the marker molecules individually to an on-state in which the molecule can emit a bunch of n photons in a row.[13–15] Single molecules are the smallest fluorescent spots possible; however, unlike the previous cases, their location is not known a priori. Provided there is only a single emitter in the diffraction volume, the position of every emitter can be calculated with subdiffraction precision Δx[16–22] by imaging the fluorescence light onto a camera. If background is negligible, the attainable precision Δx just depends on the resolving power of the detection optics, that is, the full width at half-maximum of the fluorescence spot ($FWHM_{xy}$) and the number of collected photons n [Eq. (1)].

$$\Delta x \approx \mathrm{FWHM}_{xy}/\sqrt{n} \qquad (1)$$

For example, fluorophores emitting on average 500 photons can be localized with a precision of less than 15 nm. The minimal distance at which similar objects can be distinguished is not automatically improved by this localization process itself, because it requires the emitters observed in a camera frame to be sparsely distributed, that is, to be further apart than the $FWHM_{xy}$, to guarantee that each spot is only generated from a single molecule. However, the markers can be arbitrarily close to each other if only one of them is emitting at a time. After recording and localizing sparsely distributed switched-on fluo-

[a] J. Fölling, Dr. V. Belov, Dr. A. Schönle, Dr. A. Egner, Dr. C. Eggeling, Dr. M. Bossi, Prof. Dr. S. W. Hell
Department of NanoBiophotonics
Max Planck Institute for biophysical Chemistry
Am Fassberg 11, 37077 Göttingen (Germany)
Fax: (+49) 551-2012506
E-mail: ceggeli@gwdg.de
mbossi@gwdg.de

[b] Dr. D. Riedel
Laboratory of Electron Microscopy
Max Planck Institute for Biophysical Chemistry
Am Fassberg 11, 37077 Göttingen (Germany)

rescence markers, they must be switched off again so that adjacent molecules can be switched on and localized. Therefore, the switching ability between two molecular states of the label, in conjunction with the fact that n photons are detected from the very same coordinate,[18] enables an improvement in the far-field optical resolution by the factor $\sqrt{n}$. The image of the object under investigation is reconstructed from a multitude of localized markers; in a way, the imaging procedure can be viewed as "stochastic scanning" or "polling" of individual molecules. Its resolution derives from the localization accuracy of each of the fluorescence spots. A mere overlap of the raw image data of all camera frames is identical to a conventional diffraction-limited wide-field image.

Subdiffraction imaging strategies based on this stochastic single-molecule (SM) readout have been referred to as PALM,[13] STORM,[14] fPALM,[15] and PALMIRA.[23–25] The initial PALM approach synchronized the sequential camera readout to the switching-on and in particular to the switching-off process (e.g. given by photobleaching), which resulted in long image acquisition times of up to hours. In PALM, the long acquisition time partially demanded the use of total internal reflection schemes in order to suppress ambient background. By contrast, PALMIRA uses an asynchronous acquisition mode in which readout and photoswitching are independently operated. Besides, the camera frame time is matched to the average on-time of the fluorescent marker. Values of down to 2 ms at almost 100% duty cycle enable acquisition times of about 1 min for meaningful images.[23–25] The faster image acquisition alleviates the requirement for mechanical stabilization and reduces background during readout. As a result, total internal reflection settings are obsolete, and measuring whole fixed cells has become possible.[24,25] However, the super-resolution described by Equation (1) has been applied only in the focal plane (i.e. 2D resolution). Also, the huge gain in lateral resolution is in stark contrast with the fairly poor resolution of the method in the axial direction.

The performance of a fluorescence "nanoscope" based on switchable SM detection depends on strict control of the switching-on and -off processes. In particular, it is important to switch off virtually all the markers after they have been read out. To this end, it is necessary to have compounds with an extremely low fraction of molecules that spontaneously reside in their on-state. Ideally, one should also be able to address each process independently; crosstalk between switching on (activation), readout (fluorescence generation), and switching off (deactivation) should be minimal. Although they can be individually addressed in two-color nanoscopy,[26,27] the photoswitchable fluorescent markers that have been used so far, for example, the photoswitchable protein EosFP,[13] the organic dye cyanine 5,[14,26,27] the photoactivatable green fluorescent protein (PA-GFP),[15] and the reversibly switchable fluorescent protein (RSFP) rsFastLime,[23,24,26] still need to be improved in terms of crosstalk and photon yield.

The introduction of a rhodamine amide as an effective probe for SM photoswitching "fluorescence nanoscopy" has been shown to overcome most of these issues.[25] It yields a large number of fluorescence photons that allows localization precision down to 10 nm. In addition, activation can be performed either in the ultraviolet with a single UV photon or by a two-photon absorption (2PA) process.[28] Activation by 2PA is the most striking property of the photochromic rhodamine, and it endows the technique with axial optical sectioning. In its initial realization,[25] near-infrared picosecond pulses provided by an inherently complex, mode-locked titanium–sapphire laser were used to switch on the markers by 2PA. However, under strong focusing conditions, as encountered with high-aperture objective lenses, 2PA is also possible with continuous wave (CW) illumination, as has been demonstrated in ordinary two-photon excitation fluorescence microscopy.[29] Moreover, since the labels need only be switched on sparsely, SM localization microscopy inherently relies on low fluorescence activation rates, and this makes the combination of CW illumination with 2PA highly synergistic.

Here we report nanoscale resolution in the focal plane of a far-field fluorescence microscope by using 2PA-induced photoswitching of single molecules with a CW laser. The attained lateral resolution reaches down to 13 nm. Regardless of whether pulsed or simple and cost-effective CW light is used, 2PA endows this nanoscale imaging mode with the capability for axial optical sectioning with a thickness of about 650 nm. To optimize 2PA-induced photoswitching, a novel photochromic rhodamine marker was designed, with an increased activation cross section in the deep-blue range that inherently is also more accessible to 2PA in the red or far-red. Furthermore, the novel rhodamine is relatively stable and provides high localization precision, pronounced contrast between the two photochromic states, and the possibility to drive virtually all the markers to the dark state after fluorescence emission.

Results and Discussion

Rhodamines are stable fluorescent dyes that are commonly used as fluorescent labels in far-field fluorescence microscopy (Figure 1). Derivatization of the free carboxyl group with a primary amine gave a rhodamine amide that rearranged to a final product with formation of a five-membered ring. The additional five-membered ring breaks the extended conjugation, and thus a colorless and nonfluorescent adduct is formed. The amine we have selected, a 4-aminophthalimide derivative, has two important features. First, it provides absorption in the near-UV, where conventional optics has fair transmission. Second, the imide nitrogen atom provides a branching point to introduce extra functionality depending on the group X selected (Figure 1). On the other hand, selection of the initial rhodamine compound determines most of the photophysical properties of the final fluorophore, such as the fluorescence quantum yield, the emission maximum, and so on.

Rhodamine amides are well known to be photochromic (Figure 1).[30] Irradiation of the closed isomer (CI) by UV light results in transient formation of a colored and brightly fluorescent open isomer (OI). The reaction is thermally reverted (OI → CI) with a characteristic time ranging from milliseconds to minutes, strongly dependent on the nature of the solvent.[31] Irradiation of the OI in the green range excites fluorescence emis-

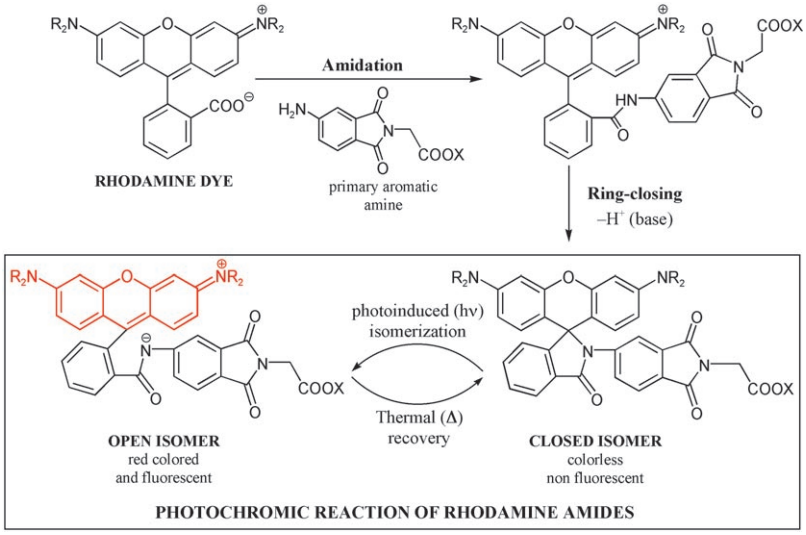

Figure 1. Photochromic reaction of rhodamine amides (light-induced ($h\nu$) activation of fluorescence, open isomer), and thermal (Δ) ring closure to the deactivated state (closed isomer). The parent rhodamine compound and the chemical modification leading to the marker used in this work are also shown.

sion but does not result in the regeneration of the CI. Thus, the fluorescent signal can be read out without an undesired erasing effect.

We recently reported a fluorescent probe based on Rhodamine B (PC-RhB, Figure 2), which results in a bright and stable marker.[25] Its photoinduced reaction can be performed with wavelengths of 375 nm for one-photon absorption (1PA) and about 750 nm for pulsed 2PA. An attempt to switch on the fluorescence of PS-RhB by CW 2PA at 670 nm was unsuccessful, and very poor activation was observed at 647 nm, which is insufficient to be used for imaging purposes. Therefore, we have designed a new marker (PC-Rh590) with a more red-shifted absorption of the OI, starting from Rhodamine 590 (Figure 2).

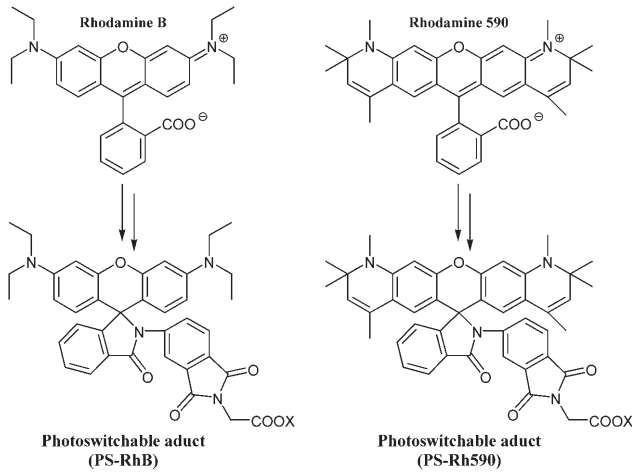

Figure 2. Photochromic rhodamine amide derivatives prepared from Rhodamine B (left) and Rhodamine 590 (right). Two kinds of derivatives were prepared: water-soluble lithium salts ($X = Li^+$), and amino-reactive NHSS esters ($X = N$-hydroxysulfosuccinimide).

The extra double bond and the rigid framework in PC-Rh590 give a considerably red shifted absorption as compared to the PC-RhB analogue (Figure 3 A), and this resulted in a more than ninefold higher efficiency of photoactivation at 375 nm (inset). The emission maximum of PC-Rh590 is also red-shifted by about 35 nm with respect to that of PC-RhB. More importantly, the new compound exhibited effective CW 2PA at 647 nm. Figure 3 B shows the results obtained for both compounds in a PVA film doped with the lithium salts ($X = Li$).

PC-Rh590 exhibited a similar photochromic behavior to the Rhodamine B derivative in terms of thermal recovery, good brightness of the emitting isomer (OI), virtually infinite contrast between the two states, and a very inefficient spontaneous ring-opening reaction (CI→OI) in comparison with its photoinduced counterpart. In the dark, only a fraction of about 1/10 000 molecules is present in the emitting OI state, as measured in a thermally equilibrated PVA film containing PC-Rh590 (Li salt). Owing to its improved activation cross section, the novel photochromic Rhodamine PC-Rh590 has excellent prospects for its use in fluorescence nanoscopy based on photoswitching, detection, and localization of single molecules.

The next step is to optimize the recording scheme of SM switching nanoscopy for PC-Rh590. Let us briefly summarize the different approaches. In principle, two recording schemes can be adopted with rhodamine amides (Figure 4), which are also generally useful for any other photoactivatable/photoswitchable fluorescence marker. In the first (gray box), the markers are activated and irreversibly bleached during readout by applying a high excitation intensity, in order to ensure a short on-time and to avoid spreading the same SM event over several camera frames. The second (dashed box) entails activation of the markers (CI→OI) and a low excitation intensity or a brief readout time followed by a lag period (on the order of the characteristic spontaneous relaxation time of the rhodamine amide). In this way, only a small fraction of markers is bleached, and the localized markers are allowed to return to the CI state to be localized again.

Each recording scheme has its advantages and drawbacks. The irreversible version yields the fastest image-acquisition times because applying large excitation intensities can push the on-time (and thus camera frame time) to less than milliseconds. Further, higher resolution is expected because the large excitation intensity extracts the maximum number of photons from each marker.[32] The reversible scheme can only be applied in polar environments where the thermal relaxation

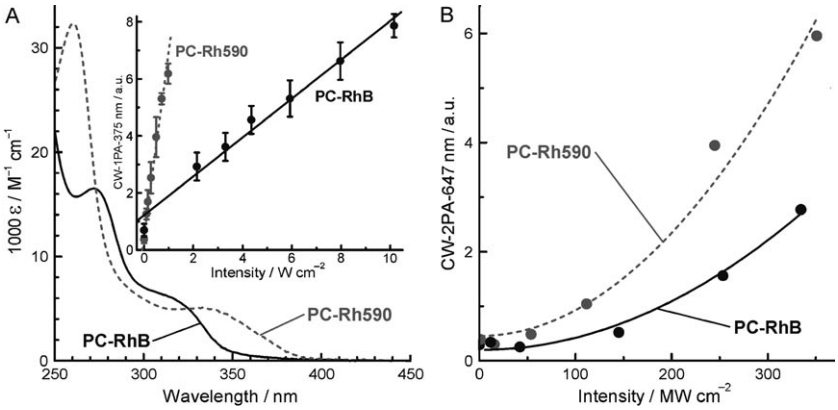

Figure 3. A) Absorption spectra of the closed isomer of the switchable rhodamine lithium salts PC-RhB (full line) and PC-Rh590 (dashed line) in aqueous solutions. The inset shows the photoinduced ring-opening reaction (see Figure 1) as a function of light intensity at 375 nm (one-photon regime) of the same compounds in PVA films. B) Intensity dependence of the same reaction with CW light of 647 nm (two-photon regime) for the same PVA films together with a squared-intensity fit to the data (lines). The extent of the photoactivation reaction (abscissa), with both 1PA (inset in A) and 2PA (B), was measured as the average number of SM detected per frame, under irradiation with the corresponding light intensity. For fair comparison, PVA films of the same thickness (40 nm) and containing the same amount of the corresponding dye were used.

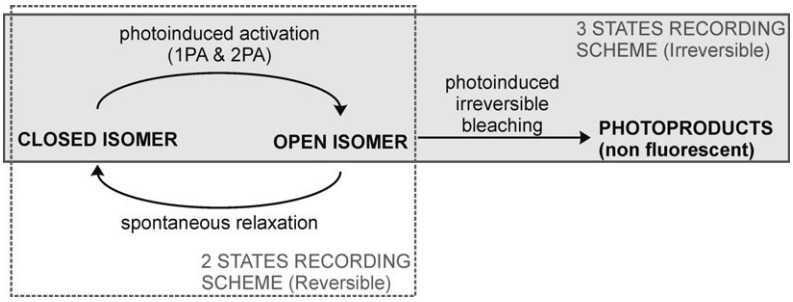

Figure 4. Two possible recording schemes for rhodamine amides in SM localization microscopy: a reversible scheme (dashed box) based on the use of the two photochromic isomers, and an irreversible one (gray box) incorporating a third photobleached state.

(OI→CI) of the rhodamine amides takes place in about 20–100 ms,[31] and thus slightly longer acquisition times result. Although there is a trade-off in the number of photons detected per SM and therefore a lower localization precision, each marker can be localized several times, that is, multiple measurements of the same marker molecule can be made. This is particularly useful for dynamic experiments in which several images must be acquired sequentially. In both recording schemes, continual acquisition of SM snapshots with a camera frame time on the order of the on-time of the OI results in the shortest possible total image-recording time. This continuous asynchronous readout complies with the PALMIRA image acquisition mode.[23,24] Since we aim at pushing our recordings to the nanoscale at the shortest possible image-acquisition time, we applied the first irreversible recording scheme in combination with continuous PALMIRA acquisition.

Fluorescence Imaging

Small core–shell silica beads were imaged by switching on PC-Rh590 markers with 375 nm light (1PA) in a wide-field microscope. Figure 5 shows a typical image of a monolayer of particles, obtained from 45 000 frames (ca. 7 min total recording time). The beads can be clearly resolved in the 1PA-PALMIRA image (Figure 5 A), while in its conventional wide-field counterpart (Figure 5 B) neither particles nor any other details can be resolved. The fluorescence image also reflects the size distribution of the beads, and reveals the presence of dumbbells and triplets. Differences in bead size appear more evident as differences in brightness. The minimal distance found between two adjacent beads is 120 nm (center to center), which is in good agreement with the average size found by transmission electron microscopy (118 nm, Figure 5 C). The mean number of photons detected per single molecule in Figure 5 was about 650, which, according to Equation (1) gives an average localization accuracy $\overline{\Delta x}$ of about 13 nm. The resulting image resolution is as good as with the previously[25] applied rhodamine amide PC-RhB, and thus our novel chemical design is similarly suited for SM switching nanoscopy. The super-resolution image (Figure 5 A) was reconstructed by plotting an area-normalized Gaussian intensity distribution with $FWHM_{Gauss}$ equal to Δx [Eq. (1)] for each detected event at its fitted centroid position.[13] Therefore, events with a low/high number of detected photons n resulted in a wider/narrower spot in the reconstructed image, which accounts for their lower/higher lo-

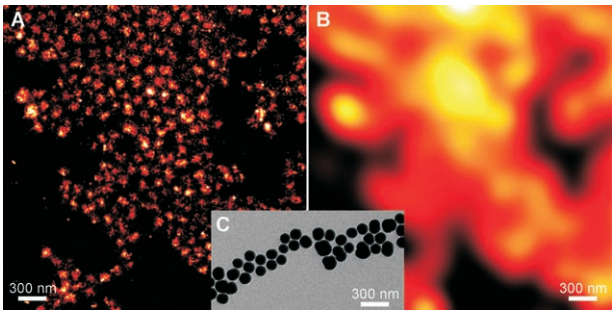

Figure 5. A) 1PA-PALMIRA image of small core–shell silica beads stained with PC-Rh590 spread on a glass substrate. B) Counterpart conventional image after linear deconvolution (see text), obtained by adding all camera frames recorded. C) TEM image of the core–shell particles at the same scale.

calization accuracies. The wide-field image (Figure 5B) was generated as an overlap of all the recorded frames (pixel size 96 nm), after background subtraction. For comparison, it was linearly deconvoluted with the point-spread function of the microscope ($FWHM_{xy} = 270$ nm) and smoothed to the same pixel size of the super-resolution image.

Switching on the marker by 2PA is restricted to a layer[28] on the order of the axial FWHM of the diffraction spot. Therefore, axial stacks (sections) can be recorded by sequentially switching on and off lateral (x,y) planes in the sample. The axial resolving power is defined by $FWHM_Z$ of the axial profile of the 2PA probability, typically about 650 nm, while the lateral resolution is given by the localization accuracy of individual PC-Rh590 molecules. Due to its quadratic intensity dependence, 2PA-induced activation requires strong focusing. For this reason, we continuously scanned the sample with a CW 647 nm laser spot (up to 350 MW cm^{-2}) during image recording. Surface-stained silica beads (5 μm in diameter) were imaged at different axial (z) positions with a spatial separation of 330 nm. Figure 6 shows a 3D reconstruction from 16 slices. The localization procedure used to assign detected events and to construct the super-resolution image of each slice is described elsewhere.[23,24] Again, highly detailed images were obtained in each slice (Figure 6B,C); this demonstrates negligible activation of out-of-plane molecules, along with the feasibility of applying nanoscale 2PA-PALMIRA microscopy in thick samples (several micrometers). The sectioning capability is as good as for pulsed 2PA,[25] which shows the success of applying simple CW laser sources for fluorescence nanoscopy with optical sectioning.

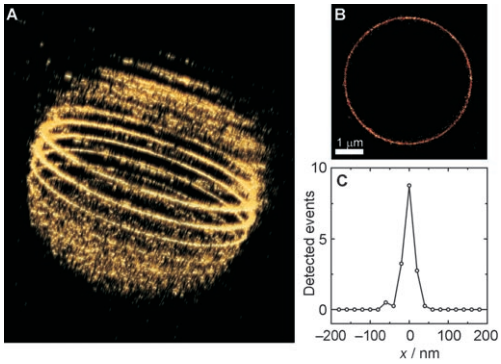

Figure 6. CW2PA-PALMIRA image of a 5 μm silica bead stained only on the surface with PC-Rh590. A) 3D reconstruction from 16 stacks. B) A layer recorded approximately at the center of the particle. C) Line profile obtained from image B) (FWHM ≈ 30 nm, pixel size = 20 nm).

Conclusions

We have demonstrated fluorescence nanoscopy with optical sectioning using two-photon induced photoswitching of individual molecules with a CW beam. Our results divulge a simple and cost-effective way of gaining optical sectioning in fluorescence nanoscopy. They have been enabled by the design and implementation of a novel organic marker, a derivative of Rhodamine 590, whose fluorescence can be switched on by a ring-opening reaction evoked through one- (1PA) and two-photon (2PA) absorption processes. Compared to previously described compounds suitable for 2PA-PALMIRA,[25] the marker presented here has a larger two-photon cross section at 647 nm, a wavelength for which highly intense CW lasers are commonly available. By performing the ring-opening reaction with CW-2PA, single-molecule switching-on and fluorescence detection is restricted to a thin layer in the focal plane, which allows axial discrimination that is impossible with 1PA. Another important feature of the marker is that the small fraction of thermally activated molecules minimizes the contribution of spontaneously activated out-of-plane emitters. Moreover, the large number of photons emitted by the marker per on-time resulted in a high localization accuracy of about 15 nm.

The use of CW light sources in the red region of the visible spectrum is an important simplification of the optical sectioning technique by 2PA over previous realizations involving short-pulse laser sources. The technique can be combined with maximum-likelihood procedures[33] for further improvement of the axial resolution. Also, the extension to other applications such as multicolour detection is feasible by generating other novel photoswitchable markers with different emission wavelengths that can be switched on through a CW-2PA process. Our results underscore once more the power of switchable photochromic molecules[10,34] for realizing far-field optical microscopy with spatial resolution far below the Abbe barrier, and promise new exciting insights into many scientific fields including live-cell imaging.

Experimental Section

All experiments were performed using a home-built microscope, which is schematically shown in Figure 7. The sample was mounted on a custom-built sample holder based on a manual Microblock 3-Axis Positioner (Thorlabs, Newton, NJ, USA). Fine tuning of the z position of the objective lens (PL APO 100×, 0.7–1.4, Leica Microsystems, Wetzlar, Germany) was performed with a z-axis positioner (MIPOS 4 CAP, Piezosystem Jena). The excitation light of 532 nm was provided by a DPSS laser (VERDI V10, Coherent Inc., Santa Clara, CA, USA), coupled to the setup by a fiber and cleaned up by

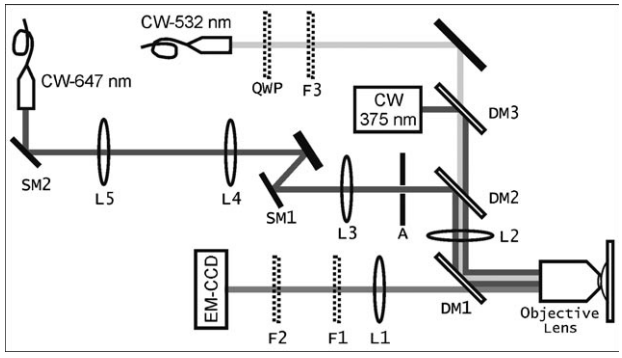

Figure 7. Schematic representation of the setup. DM1–3: dichroic mirrors; L1: tube lens, $f = 500$ mm; F1: notch filter for 532 nm; F2: fluorescence filter; EM-CCD: camera; L2, L5: lens $f = 300$ mm; L3, L4: lens $f = 80$ mm; A: square aperture; SM1, SM2: scanning mirrors, fast and slow axis, respectively; F3: laser cleanup filter, *QWP*: $\lambda/4$ waveplate. The beam path lengths are not drawn to scale.

using a laser line filter (F3, z530/10x, Chroma Technology Corp., Rockingham, VT, USA). A $\lambda/4$ waveplate (QWP) was used to obtain circularly polarized light. A diode laser (iPulse-375, Toptica Photonics AG, Gräfelfing, Germany) delivered the 375 nm activation light. The two beams were combined by using a dichroic mirror (DM3, z375 rpc, Chroma) and focused into the back aperture of the objective lens by means of lens L2, yielding a quasi wide-field illumination of about 12 μm FWHM and 18 kW cm^{-2} for the 532 nm and 50 W cm^{-2} for the 375 nm light. The two-photon activation light (647 or 671 nm) was provided by a krypton ion laser (Innova Sabre, Coherent Inc., Ca) coupled to an optical fiber. To obtain a sufficient intensity for two-photon activation, the beam was focused into the object plane and scanned over the sample. For the slow axis a piezo-actuated mirror (SM2, 30 Hz, PSH 5/2 SG, Piezosystem Jena, Germany) was used, located in the back focal plane of a 4:1 telescope consisting of lenses L5 ($f=300$ mm) and L4 ($f=80$ mm). An independently running resonant mirror (SM1, 14 kHz, EOPC, Glendale, NY, USA) was located in the focal plane of L4 and used as the fast scanning axis. The plane of SM1 was imaged into the back aperture of the objective lens by a 1:4 telescope consisting of L3 ($f=80$ mm) and L2 ($f=300$ mm). The scanning field was restricted to the field of view of the camera by means of a square aperture A, located in the focal plane of L3. A dichroic mirror DM2 (z690 sprpc, Chroma) was used to combine all three beams.

The fluorescence light was collected by the same objective and separated from the excitation and activation light by means of a dichroic mirror DM1 (z532/NIR rpc, AHF, Tübingen, Germany). It was focused onto the EM-CCD camera (IXON-Plus DU-860, Andor Technology, Belfast, Northern Ireland) by a tube lens (L1, $f=500$ mm) and separated from potential laser scattering light by using a notch filter F1 (NF01-532U-25, Semrock Rochester, NY, USA) and a fluorescence filter F2 (FF01-585/75-25, Semrock).

In all experiments the PALMIRA recording scheme (gray box in Figure 4) was used. The fast PALMIRA readout mode enabled us to perform faster measurements, and thus effectively reduced uncertainties introduced by drifting of the mechanical parts of the microscope. A frame time of 10 ms was used along with an excitation intensity close to the saturation level of the dye's fluorescence emission.[32] This adjustment ensured close-to-optimal localization accuracy and minimal background collection.[25] Usually about 10000 frames were enough to collect sufficient SM events to form meaningful images. Thus, total image acquisition times (frame time × number of frames) were only 1–2 min. Our setup proved sufficiently stable during this short period. Therefore, neither mechanical stabilization nor drift compensation was needed in any of the measurements.

Samples were prepared by spreading a suspension of silica beads, stained with the switchable fluorescent probe, in alcohol or water onto glass cover slips. Two kinds of particles were used in the experiments. Large 5 μm diameter amino-modified silica beads (Polysciences Europe GmbH, Eppelheim, Germany) were stained only on the surface with an amino-reactive (NHSS ester) modification of the fluorescent marker PC-Rh590 (Figure 2, X = *N*-hydroxysulfosuccinimide). After solvent evaporation, poly(vinyl alcohol) was spin-coated onto the beads, and the sample was covered with standard immersion oil. Small core–shell silica beads were prepared according to known protocols.[35] The dye was incorporated in the cores (74 nm diameter). A pure silica shell 22 nm thick was grown afterwards onto the cores to a total diameter of 118 nm. All sizes were determined by transmission electron microscopy (TEM). A suspension of these small particles in ethanol was evaporated onto coverslips, and no immersion fluid was added.

Acknowledgements

This work was supported by the European Commission through a Marie Curie Fellowship to M.B. and a grant within the NEST (New and Emerging Science and Technology, SPOTLITE) initiative of EU-Framework 6 to S.W.H. The marker synthesis was support by the German Ministry of Research and Education (BMBF) within the Biophotonics III programme. The authors thank K. Willig, C. von Middendorff, and C. Geisler for helpful assistance.

Keywords: dyes/pigments · fluorescence microscopy · fluorescent probes · photochromism · photoswitching

[1] E. Abbe, *Arch. Mikrosk. Anat.* **1873**, *9*, 413–420.
[2] S. W. Hell, *Opt. Commun.* **1994**, *106*, 19–22.
[3] S. W. Hell, *Science* **2007**, *316*, 1153–1158.
[4] S. W. Hell, J. Wichmann, *Opt. Lett.* **1994**, *19*, 780–782.
[5] S. W. Hell, M. Kroug, *Appl. Phys. B* **1995**, *60*, 495–497.
[6] S. W. Hell, *Nat. Biotechnol.* **2003**, *21*, 1347–1355.
[7] M. G. L. Gustafsson, *Proc. Natl. Acad. Sci. USA* **2005**, *102*, 13081–13086.
[8] V. Westphal, S. W. Hell, *Phys. Rev. Lett.* **2005**, *94*, 143903.
[9] G. Donnert, J. Keller, R. Medda, M. A. Andrei, S. O. Rizzoli, R. Lührmann, R. Jahn, C. Eggeling, S. W. Hell, *Proc. Natl. Acad. Sci. USA* **2006**, *103*, 11440–11445.
[10] M. Hofmann, C. Eggeling, S. Jakobs, S. W. Hell, *Proc. Natl. Acad. Sci. USA* **2005**, *102*, 17565–17569.
[11] M. Bossi, J. Fölling, M. Dyba, V. Westphal, S. W. Hell, *New J. Phys.* **2006**, *8*, 275.
[12] S. Bretschneider, C. Eggeling, S. W. Hell, *Phys. Rev. Lett.* **2007**, *98*, 218103.
[13] E. Betzig, G. H. Patterson, R. Sougrat, O. W. Lindwasser, S. Olenych, J. S. Bonifacino, M. W. Davidson, J. Lippincott-Schwartz, H. F. Hess, *Science* **2006**, *313*, 1642–1645.
[14] M. J. Rust, M. Bates, X. Zhuang, *Nat. Methods* **2006**, *3*, 793–796.
[15] S. T. Hess, T. P. K. Girirajan, M. D. Mason, *Biophys. J.* **2006**, *91*, 4258–4272.
[16] N. Bobroff, *Rev. Sci. Instrum.* **1986**, *57*, 1152–1157.
[17] E. Betzig, *Opt. Lett.* **1995**, *20*, 237–239.
[18] S. W. Hell, J. Soukka, P. E. Hänninen, *Bioimaging* **1995**, *3*, 65–69.
[19] T. Schmidt, G. J. Schutz, W. Baumgartner, H. J. Gruber, H. Schindler, *Proc. Natl. Acad. Sci. USA* **1996**, *93*, 2926–2929.
[20] T. D. Lacoste, X. Michalet, F. Pinaud, D. S. Chemla, A. P. Alivisatos, S. Weiss, *Proc. Natl. Acad. Sci. USA* **2000**, *97*, 9461–9466.
[21] R. E. Thompson, D. R. Larson, W. W. Webb, *Biophys. J.* **2002**, *82*, 2775–2783.
[22] W. E. Moerner, *Nat. Methods* **2006**, *3*, 781–782.
[23] C. Geisler, A. Schönle, C. von Middendorff, H. Bock, C. Eggeling, A. Egner, S. W. Hell, *Appl. Phys. A* **2007**, *88*, 223–226.
[24] A. Egner, C. Geisler, C. von Middendorff, H. Bock, D. Wenzel, R. Medda, M. Andresen, A.-C. Stiel, S. Jakobs, C. Eggeling, A. Schonle, S. W. Hell, *Biophys. J.* **2007**, *93*, 3285–3290.
[25] J. Fölling, V. Belov, R. Kunetsky, R. Medda, A. Schönle, A. Egner, C. Eggeling, M. Bossi, S. W. Hell, *Angew. Chem.* **2007**, *119*, 6382–6386; *Angew. Chem. Int. Ed.* **2007**, *46*, 6266–6270.
[26] H. Bock, C. Geisler, C. A. Wurm, S. Jakobs, A. Schönle, A. Egner, S. W. Hell, C. Eggeling, *Appl. Phys. B* **2007**, *88*, 161–165..
[27] M. Bates, B. Huang, G. P. Dempsey, X. Zhuang, *Science* **2007**, *317*, 1749–1753.
[28] W. Denk, J. H. Strickler, W. W. Webb, *Science* **1990**, *248*, 73–76.
[29] M. Booth, S. W. Hell, *J. Microsc.* **1998**, *190*, 298–304.
[30] K. H. Knauer, R. Gleiter, *Angew. Chem.* **1977**, *89*, 116–117; *Angew. Chem. Int. Ed. Engl.* **1977**, *16*, 113–113.
[31] H. Willwohl, J. Wolfrum, R. Gleiter, *Laser Chem.* **1989**, *10*, 63–72.
[32] C. Eggeling, A. Volkmer, C. A. M. Seidel, *ChemPhysChem* **2005**, *6*, 791–804.
[33] F. Aguet, D. Van De Ville, M. Unser, *Opt. Express* **2005**, *13*, 10503–15022.
[34] S. W. Hell, S. Jakobs, L. Kastrup, *Appl. Phys. A* **2003**, *77*, 859–860.
[35] A. van Blaaderen, A. Vrij, *Langmuir* **1992**, *8*, 2921–2931.

Received: October 2, 2007
Published online on January 15, 2008

